Development of Super-Hard Materials using HRTEM

Shigeo Horiuchi, Lian-Long He*, Jianyu Huang*,
Takashi Taniguchi and Minoru Akaishi

National Institute for Research in Inorganic Materials, Tsukuba, 305, Japan
**on leave from Metal Research Institute, Chinese Academy of Sciences, Wenhua Road 72, Shenyang 110015, P.R.China*

(Received: Jan. 30, 1997 Accepted: Feb. 19, 1997)

Abstract

High-resolution transmission electron microscopy (HRTEM) reveals some new types of microstructures in the course of the phase transition from h(hexagonal)- to c(cubic)-boron nitride under high pressure (7.7GPa) at high temperature (1250~1800°C). Interplanar spacings between sp^2 sheets prominently contracts from d=3.33 to 3.10Å in so-called "compressed h-BN". This is due to a monoclinic lattice distortion of residual h-BN, which originates from the difference in the compressibility as well as the thermal expansion between adjoining h- and c-BN grains. Thin plates of h-BN are often folded and the folding also induces the monoclinic phase. At the edge of h-BN plates sp^2 sheets roll up to form semispiral rod-like t-BN with an average interplanar spacing of 3.5Å. That w(wurzite)-BN is partly included in a small c-BN grain suggests that w-BN firstly appears at the initial stage of phase transition and is then replaced by nano-twinned c-BN. The formation of super-hard c-BN, which is an important industrial material for cutting and polishing iron and steel products, is prominently promoted, when the starting h-BN is vibration-milled, due to the mechano-chemical effect.

1. Introduction

It is known that h- and r-BN are formed under ambient pressure. Boron and nitrogen atoms form hexagonal rings, which extend two-dimensionally in sheets, using the sp^2 B-N bond. Their crystal structures are schematically shown in Figs.1(a) and 1(b) [1,2]. Closed circles represent B atoms, and open ones N atoms. Neighboring atomic sheets are weakly bound with the interplanar spacing (d_{0002} in hexagonal notation) of 3.328 and 3.34Å for h-BN and r-BN, respectively. Their stacking sequence is conventionally represented by ab'ab' and abcabc, respectively.

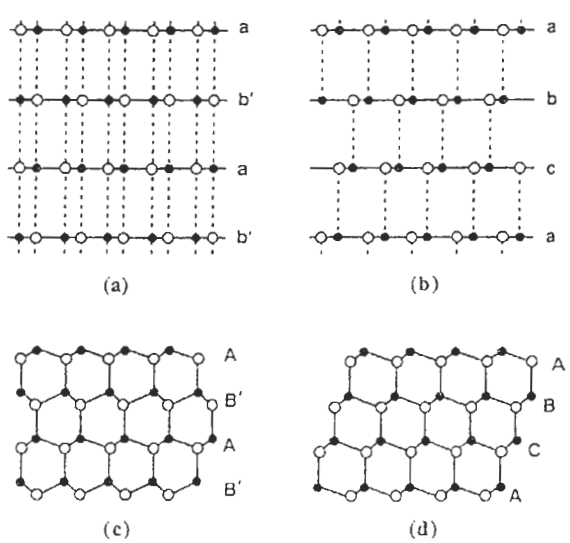

Fig. 1 Projections of the crystal structure of h-BN (a), r-BN (b), w-BN (c) and c-BN (d). ●:B and ○:N

w-BN is prepared from h-BN under high pressure at room temperature [3]. The interplanar spacing becomes small (d_{0002}=2.211 Å), i.e. B and N atoms are bound by the sp^3 bond and cause the sheets to be puckered (Fig.1(c)) [4]. The sequence of the puckered sheets is represented by AB'AB'. For the structure of c-BN (Fig.1(d), d_{111}=2.087Å) the stacking sequence is ABCABC. c-BN is the second hardest material with the hardness of half that of diamond and is used for grinding and cutting industrial ferrous materials [5]. Another prominent feature is its high thermal conductivity [6]. It is prepared from h-BN using catalysts such as $M_3B_2N_4$ (M: Mg,Ca,Sr,Ba) under moderately high pressures at high temperatures [7], while directly (without any catalysts) under very high pressures at high temperatures [3,8]. The mechanism of the transition has not been clarified yet.

In addition to the above structures, there is t(turbostratic)-BN, in which sp^2 sheets are irregularly rotated around the axis normal to the sheet or irregularly shifted translationally [9]. The interplanar spacing is slightly larger than that for h-BN or r-BN (d=3.5Å). A t-BN of tubular form has been prepared by heating amorphous BN [10].

In the present study the microstructures are examined by high-resolution transmission

electron microscopy (HRTEM). Based on the results obtained the mechanism of the phase transition will be discussed. As a result how to promote the formation of c-BN will be proposed.

2. Experimental

We have developed the first high-resolution high-voltage electron microscope (HR-HVEM, model H-1250) with the resolving power d_s=2.0Å in 1976 [11] and the second HR-HVEM (model H-1500) with d_s=1.0Å in 1991 [12]. In the present study we have used the H-1500 HR-HVEM at the accelerating voltage of 1000kV. Thin foils were prepared from bulk specimens by the so-called crushing or ion-milling method.

Commercially available hot-pressed h-BN (Denkikagaku Co. type N-1) was heated at 2100°C for 2h in a flow of N_2 gas to decrease the oxygen content down to 0.06-0.07 wt%. Each particle of the powders has a hexagonal plate form with the plate plane parallel to (0001). The size of the plate is smaller than a few μm and the thickness is less than several hundred Å. It easily becomes thinner (<100Å) by cleavage, when crushed in an agate mortar. According to HRTEM no particular lattice defects are found in the crystals. They were used as a starting material.

3. Experimental results

3.1 Identification of m-BN (compressed h-BN) [13]

An x-ray diffraction peak of so-called "compressed h-BN", which shows a slightly smaller interplanar distance (d=3.1Å) than that for the normal h-BN mentioned above, has been observed from the material obtained during the initial stages of the phase transition [6,14]. This was considered to be caused by small crystallites of h-BN trapped under the high pressures within c-BN crystals, although any microscopic evidence was not given.

The starting powders were shaped into pellets (6mmϕ×5mm) and then heated at 1800°C under a pressure of 7.7GPa for 20min, using a previously reported high pressure apparatus [15]. An x-ray diffraction chart taken from the bulk product shows that the major peaks are those from c-BN, with a very weak peak from h-BN. In addition, a substantially intense, diffuse peak of "compressed h-BN" occurs at an angle of 2θ=26.7°~29.2°(d=3.34~3.06Å) with an intensity peak at 2θ=28.4° (d=3.10Å), where θ is the scattering angle.

According to the electron microscopy results, the grains of c-BN are small (<1μm) and have no special shape. In local regions, however, several thin plates coagulate. Fig.2 shows a micrograph from such a region, in which electron beam is incident nearly parallel to the plate planes. It is noted that the thin plates are folded at many sites. Some of them are highlighted by arrows. This suggests that they are plastically deformable under high pressure and high temperature. A grain of c-BN appears in the lower right part, as marked by an asterisk.

In the corresponding diffraction pattern inserted in Fig.2, the spots are not exactly on concentric circles. This indicates that the lattice spacing is not exactly identical for each area but fluctuate to some extent. By comparing with the diffraction spots of c-BN as a reference the lattice spacing between sp^2 sheets is calculated to range from 3.4 to 3.1Å for the innermost ring. We may then say that the plate-like crystals are mainly composed of "compressed h-BN".

Fig.3 is an HRTEM image for the boundary area between the c-BN grain and the surrounding "compressed h-BN" matrix in Fig.2. Electron beam is incident almost parallel to the [1$\bar{1}$0] direction of the c-BN grain. Many thin twins with (111) boundaries are seen in the grain. Besides, w-BN is found partly in the

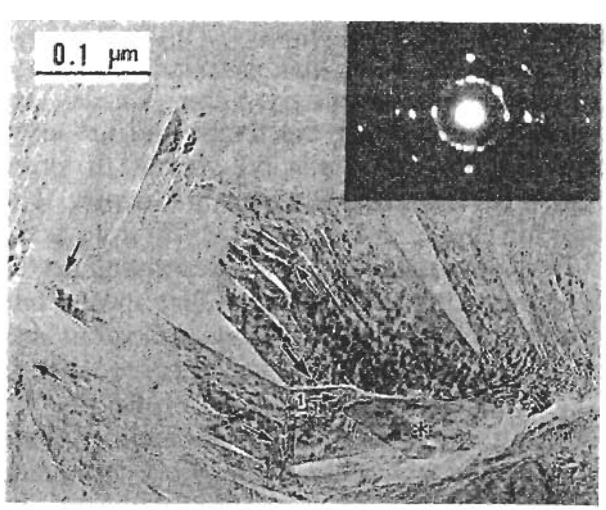

Fig. 2 An electron micrograph of thin plate-like crystals, which excite the diffraction peaks of "compressed h-BN". The plates are sharply folded at the sites of arrows. A thick arrow indicates the site, where a plate terminates, while an asterisk a c-BN grain. An electron diffraction pattern taken from the whole area is inserted.

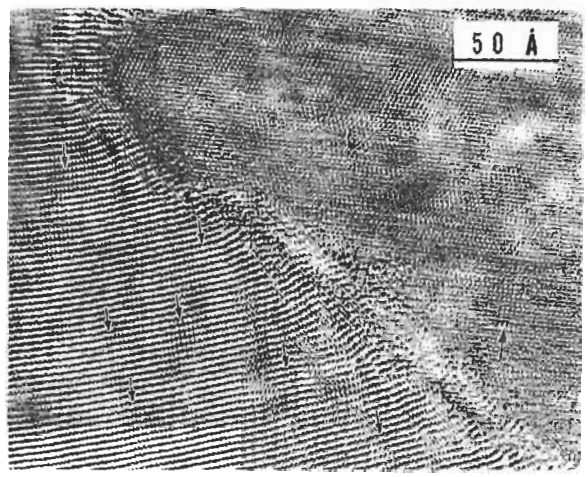

Fig. 3 An HRTEM image showing the boundary area between the c-BN grain and the surrounding "compressed h-BN", in which the lattice fringes are prominently bent. The arrangement of bright spots in areas of downward arrows shows the monoclinic lattice distortion. An upward arrow in the c-BN grain shows the coexistence of w-BN.

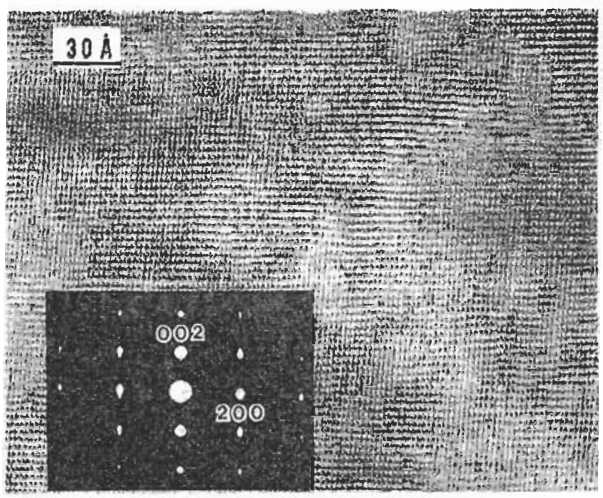

Fig. 4 An HRTEM image of the monoclinic phase, which gives the diffraction peaks of "compressed h-BN". The spots in the attached diffraction pattern are indexed based on the monoclinic unit-cell (a=4.33, b=2.50, c=3.2Å and β= 94°).

grain, as marked by an upward arrow. According to the electron diffraction pattern in Fig.2 and the HRTEM image in Fig.3 the c-BN grain has such an orientation relationship with the surrounding matrix as $[1\bar{1}0]_c$ //$([11\bar{2}0]_w$ //$)[11\bar{2}0]_h$ and $[111]_c$ //$([0001]_w$ //$)[0001]_h$.

In the surrounding matrix the lattice planes of the sp^2 sheet are prominently bending. In some areas the bright spots are resolved. According to a computer simulation of the intensity of the HRTEM images [16] the bright spot appears at the center of a pair of B and N columns, which are adjacent in the projection plane (cf.Fig.1(a)). Interestingly, the sheets are slightly sheared along the fringe and the array of spots is not rectangular but slightly distorted in the areas marked by downward arrows. The distortion angle is different for different areas but lies in the range of 5～9°, depending on the curvature of the lattice fringe. This means that the crystal symmetry is no longer hexagonal but monoclinic, although the stacking sequence is still essentially the same as that of h-BN.

Under high pressure (7.7GPa) h- and c-BN are known to be compressed by about 89% and 98%, respectively [17,18]. However, for the case of specimens, in which the two phases coexist, the volume can not be completely retrieved when the high pressure is removed, because of mutual restraint at the boundaries. This restraint must be an origin for causing the lattice bending observed above. Besides, the thermal expansion coefficient is prominently different between h- and c-BN [1,19]. This must induce the similar effect to the difference in the compressibility, and must be another origin to additionally cause the mutual lattice restraint. The interplanar spacing of the bending lattice in Fig.3 is measured to be in the range between d=3.1 and 3.4Å. In this case we have used the measured value (d_{111}=2.1Å) of c-BN as a reference.

In the leftward area of Fig.3 lattice fringes becomes rather straight and widely extends. An example of such area is shown in Fig.4. Here the monoclinic lattice distortion is always kept and the lattice spacings are measured to be about 3.2Å In the corresponding diffraction pattern attached to Fig.4 the lattice distortion as well as the contraction of the interplanar spacing is also noted clearly. From the reflection conditions obtained from a series of diffraction patterns, we can determine the possible space groups to be Cc or C2/c (monoclinic).

Fig.5 shows the relationship between the monoclinic and hexagonal lattices. The lattice parameters measured from electron diffraction patterns and HRTEM images of the monoclinic phase are slightly fluctuated according to areas and described as follows; a=4.33, b=2.50, c=3.1～3.3Å and β=92～95°. The value of c is slightly larger than that measured from the x-ray diffraction mentioned above. This must be due to the decrease in the lattice restraint inside

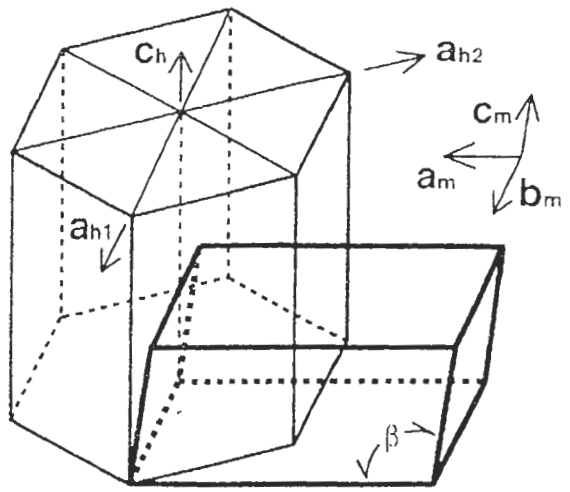

Fig. 5 A lattice relationship between h- and m-BN.

the thin specimens used for electron microscopy.

As shown in Fig.2, the plates are often folded. They change the thickness on folding. The magnitude of the change depends on the folding angle as well as the tilting angle of the folding plane. The folding is mostly due to the external stress. In some cases it is promoted by the volume shrinkage due to the formation of c-BN grains. Such an example is seen at the site of arrow 1 of Fig.2. According to HRTEM the shear of sp^2 sheets to the monoclinic lattice is clearly seen and the spacings are measured to be about 3.2Å. This indicates that the folding also serves to form the monoclinic phase.

3.2 Semispiral t-BN [20]

Fig.6 is an HRTEM image taken from an edge part of a plate, marked by a thick arrow in Fig.2. In the upper part any spot array is not obtained since the incident direction of electron beam is deviated from [1$\bar{1}$0]. The observation that the interplanar spacing is 3.3Å suggests that the plate is composed of residual h-BN, which has been detected by a weak peak of x-ray diffraction.

At the edge of the plate the sp^2 sheets roll up to form a semispiral pattern. On tilting the specimen it is noted that a nearly straight rod with a semispiral cross-section elongates in the direction normal to the photograph. This indicates that the surface plane is composed only of sp^2 sheet so that the surface energy is minimized. The interplanar distance in the semispiral area is slightly wider (d=3.3～3.9Å with an average of 3.5Å) than that in the plate. It is certain from these observations that t-BN arises in the rods. A granular pattern, being

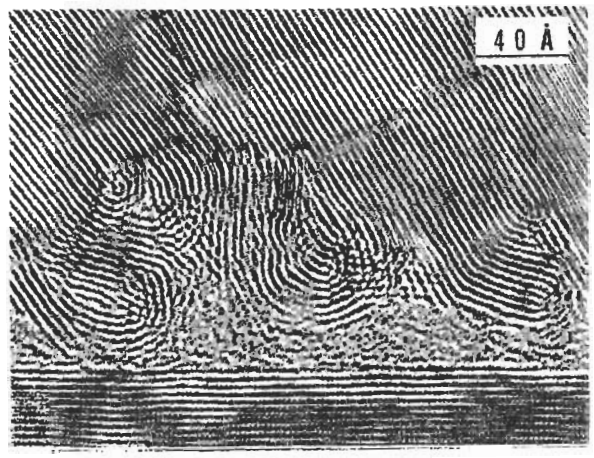

Fig. 6 t-BN rods with the cross-section of semicircular lattice, found at the edge of h-BN plate. The interplanar spacing is 3.3～3.9Å in the former and about 3.3Å in the latter. The lower part is due to the monoclinic phase.

characteristic for any amorphous substances, is seen around the rods. It has been reported that the h-BN evaporates at temperatures higher than 1750°C and recrystallizes to r-BN at lower temperatures under ambient pressure [2]. The present amorphous area is considered to be formed due to the deposition of the evaporated BN, under the high pressure and high temperature. The semicircular lattice must have been formed by atomic diffusion from the plate and/or by heating the amorphous BN [10].

3.3 Promotion of c-BN formation [21]

As mentioned above, w-BN is partly included in a small c-BN grain (Fig.3), while hardly in large c-BN grains. The most probable process of the phase transition is therefore that a small region of w-BN is firstly formed at the initial

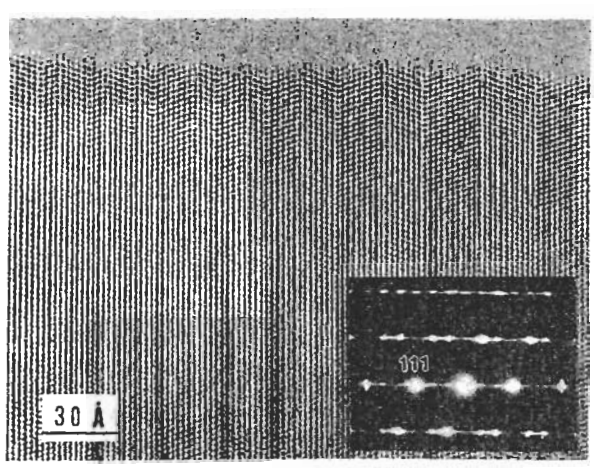

Fig. 7 HRTEM image of a c-BN grain, in which twinning occurs on a nano scale. A simulated image is inserted.

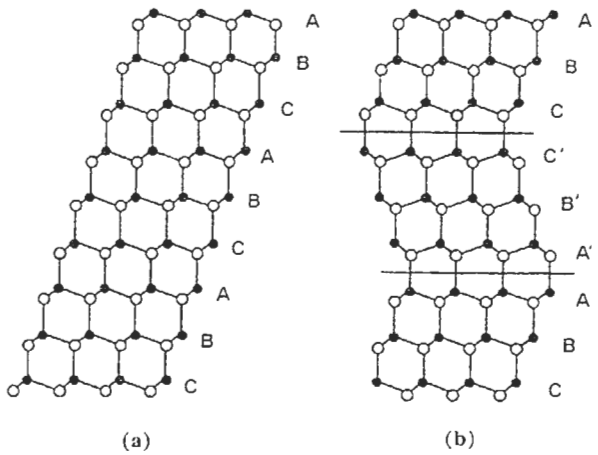

Fig. 8 A model of nano-twinning in a c-BN grain.

stage of phase transition and then converted to c-BN. On the conversion the twinning in c-BN must be necessary to decrease the strain, which would otherwise be introduced because of the difference in the crystal structure between c- and w-BN. Fig.7 is an example of nano-twins.

Fig.8 schematically shows how their formation deduces the mechanical strain.

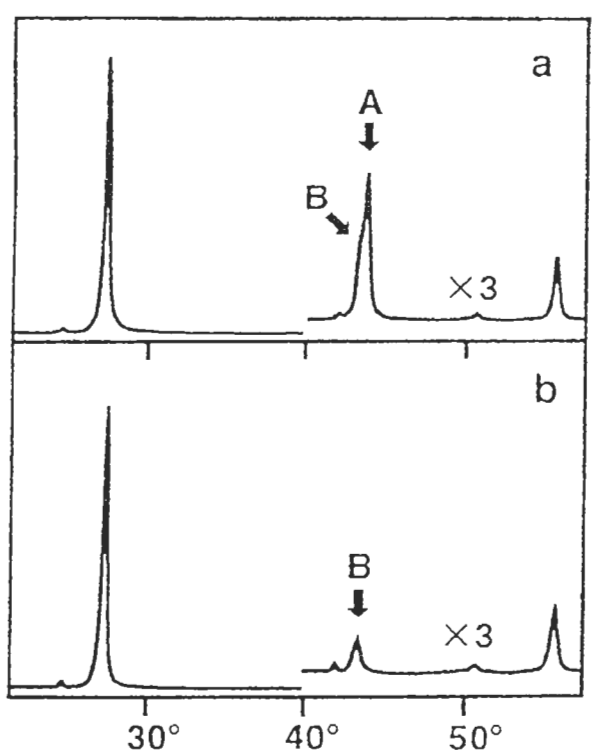

Fig.9 X-ray diffraction chart showing the promotion of c-BN formation by mechano-chemical effect. Specimens were prepared under 7.7GPa at 1350°C after vibration milling in (a), while without milling in (b). A diffraction peak is from (111) of c-BN, B from (0002) of w-BN and intense peaks from h-BN.

It has also been observed that many stacking faults are included in the w-BN. This suggests that defects in the starting h-BN plays an important role on the formation of w-BN and then c-BN. We have performed a vibration-milling to h-BN, which was further treated under high-pressure at high temperature. As a result the formation of c-BN was strongly promoted. As an example, from the specimen, which has been heated under 7.7GPa at 1350°C, x-ray diffraction peaks of c-BN are clear, while only those of w-BN are weakly detected (Fig.9). This is considered to be due to a mechano-chemical effect.

Acknowledgement

The authors would like to express sincere thanks to Drs.S.Yamaoka, M.Onoda and Y.Matsui for their valuable discussions.

References

1. R.S.Pease, Acta Cryst. 5,356(1952).
2. T.Ishii, T.Sato, Y.Sekikawa & M.Iwata, J.Cryst.Growth 52,285 (1981).
3. F.P.Bundy & R.H.Wentorf,Jr. J.Chem.Phys. 38,1144(1963).
4. M.Wakatsuki, K.J.Takano & G.Fujita, Physica 139 & 140B, 256(1986).
5. R.C.DeVries, GE Report #72 CRD 178(1972).
6. F.R.Corrigan, High Pressure Science and Technology, 6th AIRAPT Conf. vol.1, ed.by K.D.Timmenhaus and M.S.Barber (Plenum Press, New York,1979) p.994.
7. T.Endo, O.Fukunaga & M.Iwata, J.Mater.Sci. 14,1676(1979).
8. R.H.Wentorf,Jr. J.Chem.Phys. 26,956(1957).
9. J.Thomas,Jr., N.E.Weston & T.E.O'Connor, J.Am.Chem.Soc. 84, 4619(1963).
10. E.J.M.Hamilton, S.E.Doran, C.M.Mann, H.O.Colijn, V.A.McDonald & S.G.Shore, Science 260, 659(1993).
11. S.Horiuchi, Y.Matsui and Y.Bando, Jpn.J.Appl.Phys. 15,2483(1976).
12. S.Horiuchi, Y.Matsui, Y.Kitami, M.Yokoyama, S.Suehara, X.J.Wu, I.Matsui and T.Katsuta, Ultramicroscopy 39,231(1991).
13. S.Horiuchi, L.L.He, M.Onoda & M.Akaishi, Appl.Phys.Lett.69,182(1996).
14. F.R.Corrigan & F.P.Bundy, J.Chem.Phys. 63,3812(1975).
15. M.Akaishi, T.Sato, M.Ishii, T.Taniguchi &

S.Yamaoka, J.Mater.Sci.Lett. 12,1883(1993).
16. S.Horiuchi, Fundamentals of High-Resolution Transmission Electron Microscopy (North-Holland, Amsterdam, 1994), p.211.
17. R.W.Lynch & H.G.Drickamer, J.Chem.Phys. 44,181(1966).
18. E.Knittle, R.M.Wentzcovitch, R.Jeanloz & M.L.Cohen, Nature 337, 349(1989).
19. G.A.Slack & S.F.Bartram, J.Appl.Phys. 46,89(1974).
20. S.Horiuchi, L.L.He & M.Akaishi, Jpn.J.Appl.Phys.34,L1612(1995).
21. S.Horiuchi, L.L.He, T.Taniguchi, Rev.High Pres.Sci.Tech.(Spe.Issue) 5,226(1996).